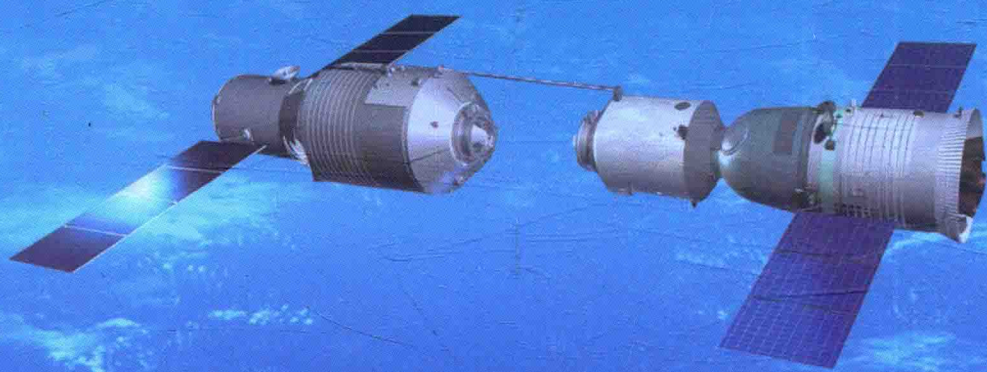


航天器机构 及其可靠性

(第二版)

刘志全 等著



中国宇航出版社

航天器机构及其可靠性

(第二版)

刘志全 等著



中国宇航出版社

·北京·

内 容 简 介

第二版在第一版的基础上,补充了球铰接杆式支撑臂、空间柔性机械臂、月球钻取式采样机构、空间聚光电池阵菲涅耳透镜和太阳翼黏滞阻尼器等相关内容。

本书涵盖了“机械基础——零部件设计与分析”、“航天器机构的发展”、“航天器机构的设计与分析”和“航天器机构可靠性设计、试验及评估”四部分内容,不特别追求对机构基础理论描述的系统性和对机构种类覆盖的全面性,而力求突出航天器机构个性化的创新性研究成果。

作者以航天器机构工程研制经验为基础,总结了20多年来作者及有关合作者在部分机械零部件、航天器机构及其可靠性方面的研究成果,撰写成本书。

本书可供高等院校相关专业师生及航天器相关领域工程技术人员参考。

版权所有 侵权必究

图书在版编目(CIP)数据

航天器机构及其可靠性/刘志全等著. -- 2版. --

北京:中国宇航出版社,2015.12

ISBN 978-7-5159-1045-1

I. ①航… II. ①刘… III. ①航天器—机构学—可靠性 IV. ①V423

中国版本图书馆CIP数据核字(2015)第300533号

责任编辑 彭晨光 封面设计 宇星文化

出版 中国宇航出版社
发行
社址 北京市阜成路8号 邮编 100830
(010)60286808
网址 www.caphbook.com
经销 新华书店
发行部 (010)60286888 (010)68371900(传真)
(010)60286887 (010)60286804(传真)
零售店 读者服务部 北京宇航文苑
(010)68371105 (010)62529336
承印 北京国中画印刷有限公司

版次 2015年12月第2版
2015年12月第2次印刷
规格 787×1092
开本 1/16
印张 30.75 彩插 8面
字数 668千字
书号 ISBN 978-7-5159-1045-1
定价 98.00元

本书如有印装质量问题,可与发行部联系调换

第二版前言

随着航天事业的发展，航天器的功能不断增强，性能不断提高，越来越多的机构被应用到航天器上。航天器机构的可靠性问题也越来越突出。为了进一步提升航天器机构的设计水平，提高航天器机构的可靠性，促进研究成果应用于航天器工程，作者以航天器机构工程研制经验为基础，总结了作者20多年来在部分机械零部件、航天器机构及其可靠性方面的研究成果，撰写成《航天器机构及其可靠性》这本书，并于2012年12月出版了第一版。

第二版在第一版的基础上，补充了球铰接杆式支撑臂、空间柔性机械臂、月球钻取式采样机构、空间聚光电池阵菲涅耳透镜和太阳翼黏滞阻尼器等相关内容。

本书涵盖了“机械基础——零部件设计与分析”、“航天器机构的发展”、“航天器机构的设计与分析”和“航天器机构可靠性设计、试验及评估”四个部分的内容，不特别追求对机构基础理论描述的系统性和对机构种类覆盖的全面性，而力求突出航天器机构个性化的创新性研究成果。

本书的出版得到了中国空间技术研究院总体部王永富研究员、范含林研究员、柴洪友研究员及中国宇航出版社的支持与帮助，作者在此谨致谢意。中国空间技术研究院总体部的官颖、孙国鹏和李新立3位高级工程师及王丽丽博士参加了本书的校对和修改工作，在此一并感谢。

本书可供高等院校相关专业师生及航天器相关领域工程技术人员作为参考。

欢迎读者对本书中的错误和疏漏之处给予批评指正。

作者

2015年10月

目 录

第 1 篇 机械基础——零部件设计与分析

Research on Cone Tooth Spherical Gear Transmission of Robot Flexible Joint	3
机器人柔性关节准椭球面齿轮传动——节曲面的优化设计	12
机器人柔性关节准椭球面齿轮传动——齿形分析与设计	20
高速轴承结构和性能的发展	27
滚动轴承油膜厚度及运动参数的测试	30
线接触弹流理论研究的三个方面	34
Parameter Measurement of 4010 Synthetic Aviation Lubricant	41
高速圆柱滚子轴承的热分析模型	51
高速圆柱滚子轴承温度分布的计算与测试	57
某直升机齿轮传动系统的稳态热分析	65
某直升机齿轮传动系统的瞬态热分析	73
航空发动机轴承腔热状态分析模型及温度场计算	79
高速滚动轴承在失去润滑情况下工作游隙的计算方法	86

第 2 篇 航天器机构的发展

空间对接组件中的结构锁及其传动系统	95
载人航天器舱门机构原理与特点分析	103
月球探测器软着陆机构发展综述	113
载人航天器舱门周边传动锁紧释放机构的原理与特点	122
空间光学遥感器的主镜展开机构	128
构架式空间可展开支撑臂	136
深空探测自动采样机构的特点及应用	144
空间太阳能电池阵的发展现状及趋势	152
载人航天器柔性机械臂的动力学建模方法	162

第 3 篇 航天器机构的设计与分析

空间对接机构结构锁的优化设计	175
带有偏心轮的锁钩式结构锁运动性能和力分析	185
载人航天器电动兼手动舱门的研究	196
载人航天器舱门有限元分析及机构最小传动角计算	205
月球探测器软着陆机构展开过程的运动学分析	213
一种空间光学遥感器的主镜展开机构	222
空间光学传感器主镜展开机构重复定位精度分析	229
空间光学传感器主镜展开机构锁紧刚度分析	239
球铰接杆式支撑臂构型参数分析	246
球铰接杆式支撑臂展开过程中横向振动分析	254
球铰接杆式支撑臂斜拉索组件的参数影响分析	269
月面钻取式自动采样机构的设计与分析	279
钻取式自动采样机构螺旋钻杆结构参数的多目标优化	289
月球钻取采样钻头结构参数对力学性能的影响	302
空间聚光电池阵用拱形菲涅耳透镜的设计与分析	315
基于线聚焦菲涅耳透镜的空间聚光光伏系统特性的实验研究	328
空间聚光太阳电池阵柔性透镜薄膜结构的力学分析	340
空间机械臂关节精细动力学模型的建立及关节力矩控制	354
柔性机械臂辅助空间站舱段对接阻抗控制	364

第 4 篇 航天器机构可靠性设计、试验及评估

航天器机构可靠性设计的若干要素	375
航天产品 FMEA 工作有效性的思考	381
航天器机械可靠性特征量裕度的概率设计方法	387
航天器机构的可靠性试验方法	398
航天器火工机构的可靠性验证试验及评估方法	406
长寿命航天器机构的加速寿命试验方法	413
航天器机构固体润滑球轴承磨损失效模型	422
航天器机构固体润滑球轴承的加速寿命试验方法	429
载人飞船座椅缓冲机构的可靠性试验方法	438
载人航天器密封舱门的可靠性验证试验方法	445

载人飞船某连接分离机构的可靠性验证试验方法	451
航天器开关类机构可靠性验证试验方法	458
航天器太阳翼展开可靠性的评估方法	464
太阳翼黏滞阻尼器的可靠性评估方法	470
火工切割器的一种小样本可靠性验证试验	476

第 1 篇

机械基础——零部件设计与分析

Research on Cone Tooth Spherical Gear Transmission of Robot Flexible Joint*

Liu Zhiquan Li Guixian Li Huamin

Abstract: This paper studies the principles of cone tooth spherical gear transmission of robot flexible joint, and also analyses and calculates the profile of convex tooth and concave tooth.

Keywords: cone tooth spherical gear transmission

INTRODUCTION

Robot flexible wrist is the end of robot action. Its flexibility and movement range greatly affect the robot performance as a whole. So experts and scholars working on robot research both at home and abroad pay much attention to the research of robot flexible wrist. The spherical gear transmission (shown in Fig.1) invented by a Russian, A. H. Куклин has been successfully applied to the robot wrist made in Norwegian Trallfa Company—a wrist much welcomed internationally. Document [1] analysed the gear meshing of the spherical gear transmission of this wrist. This wrist joint is in fact a space gear-connecting rod mechanism. Its simple figure is shown as Fig. 2

In the two pairs of spherical gears, the gear ratio of one pair is 1, but the gear ratio of another pair is not 1. It makes the transmission of variable gear ratio in the longitude direction. The tooth profile of these two pairs of gears is the rotation surface of involute (see also [1]). To the spherical gear transmission whose gear ratio is not 1, because the sizes of two pitch spheres are not the same, it is impossible to make sure their latitude arc lengths (pitch) correspondingly equal when they make sure their longitude arc lengths (pitch) equal. In order to realize the transition from one pitch sphere to another, the pitch surface has to become stepping concentric sphere, and tooth profile will have some proper modification. This inevitably affects the operation performance of gears. Document [2], directed against the problems remaining in the spherical gear transmission whose gear ratio is not 1, studied the quasi-ellipsoid gear transmission which used the smooth quasi-

* 1990 ASME Design Technical Mechanism Conference—21st Biennial Mechanism Conference, Chicago, Illinois, Sept. 16-19, 1990. DE-Vol. 26, pp419-422. EI: 1991020082933

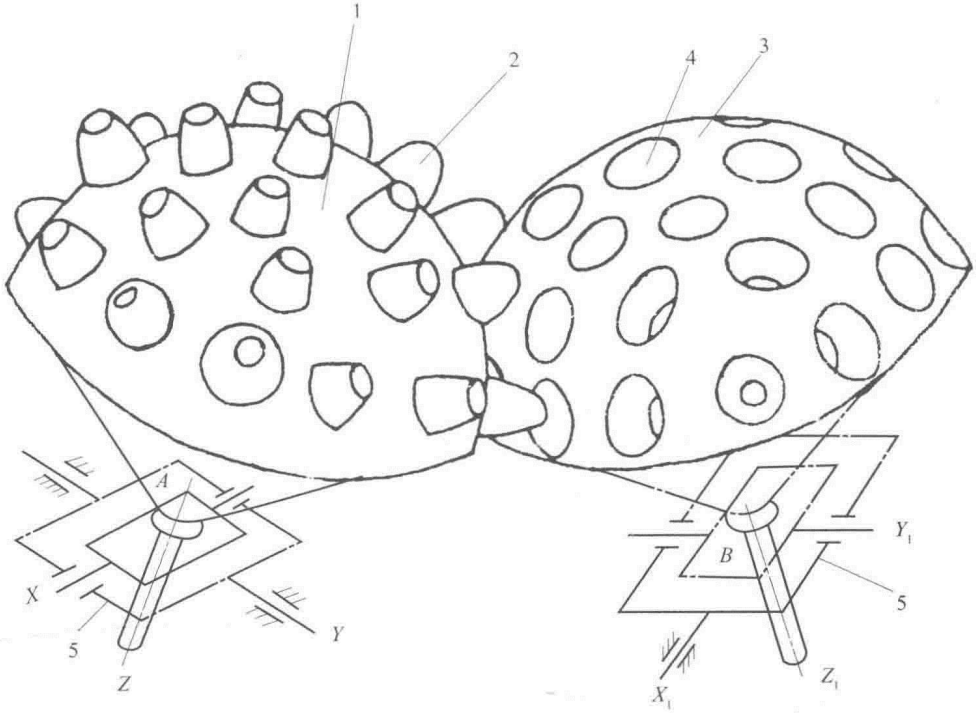


Fig. 1 Spherical gear transmission

ellipsoid pitch surface instead of stepping concentric sphere surface and also made some improvement on tooth profile. On the basis of analysing the principles of the spherical gear transmission, this paper deals with that pair of spherical gear transmission whose gear ratio is 1, presents a new kind of tooth profile i. e. cone tooth instead of the involute rotation surface tooth profile which was adopted in the past, and studies this new kind of tooth profile.

1 THE PRINCIPLES OF SPHERICAL GEAR TRANSMISSION OF ROBOT FLEXIBLE JOINT

As shown in Fig. 2, 1-2 and 3-4 are respectively the two pairs of spherical gears. The rest all belongs to the frame work. A, C, D are all the intersection points of cross-shafts. The movements of the three degrees of freedom of flexible joint are the pitching movement around shaft X, the yawing movement around shaft Y, and the rolling movement around shaft Z. The so-called whole position bending is just the pitch-yaw compound motion of all kinds in different positions. Its bending extent depends on the travel of the cylinder pusher bars.

Take the two sphere crowns with different sphere centres as pitch surfaces; Take the

sphere centres of these two sphere crowns respectively as two different rotation centres; Distribute convex teeth and concave teeth which can mesh each other respectively on the two spherical surfaces. This forms the spherical gear transmission, shown in Fig. 1.

In fact, the so-called rotation centres are intersection points of cross-shafts which are vertical with each other of the frame work. It is just like spherical hinge. As far as the spherical gear transmission whose gear ratio is 1 is concerned, the movement relation of this set of space gear-connecting rod mechanism can be completely simplified as the movement relation concerned in the epicyclic gear train (shown in Fig. 3) when the joint bends in one certain position in the limited space, because the bending movements of the flexible joint in all positions are all the same.

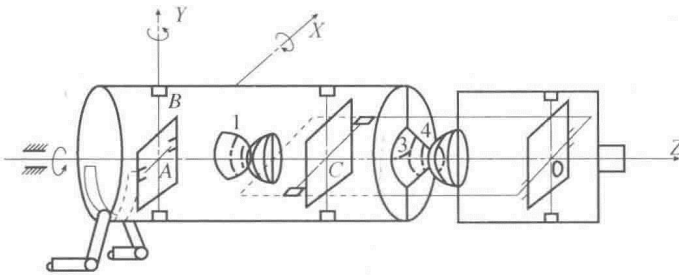


Fig. 2 A robot flexible wrist with two pairs of spherical gears

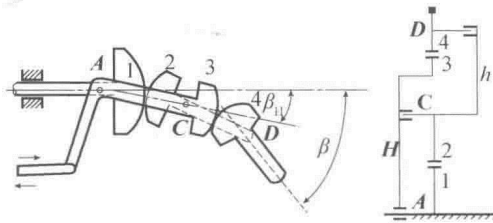


Fig. 3 Gear transmission principle

According to the Willis method

$$i_{12}^H = \frac{-\omega_H}{\omega_h - \omega_H} = -\frac{r_2}{r_1} \quad (1)$$

$$i_{34}^h = \frac{\omega_3^H - \omega_h^H}{\omega_4^H - \omega_h^H} = \frac{-(\omega_h - \omega_H)}{(\omega_4 - \omega_H) - (\omega_h - \omega_H)} = -\frac{r_4}{r_3} \quad (2)$$

Combine (1) and (2), we can obtain

$$i_{4H} = \frac{\omega_4}{\omega_H} = 1 + i_{21}(1 + i_{43})$$

i. e. $\omega_4 = [1 + i_{21}(1 + i_{43})]\omega_H \quad (3)$

Formula (3) is the movement relation between the hand 4 and planet carrier H.

2 THE DISTRIBUTION OF TEETH

In the spherical gear transmission whose gear ratio is 1, the radii of two pitch spheres are the same and convex teeth match concave teeth one by one, so the distributions of convex teeth and concave teeth are all the same. In order to make the longitude pitch equal to the latitude pitch as much as possible, we can use the geometrical condition of the spherical equilateral triangle to distribute the teeth evenly on the pitch sphere, shown in Fig. 4.

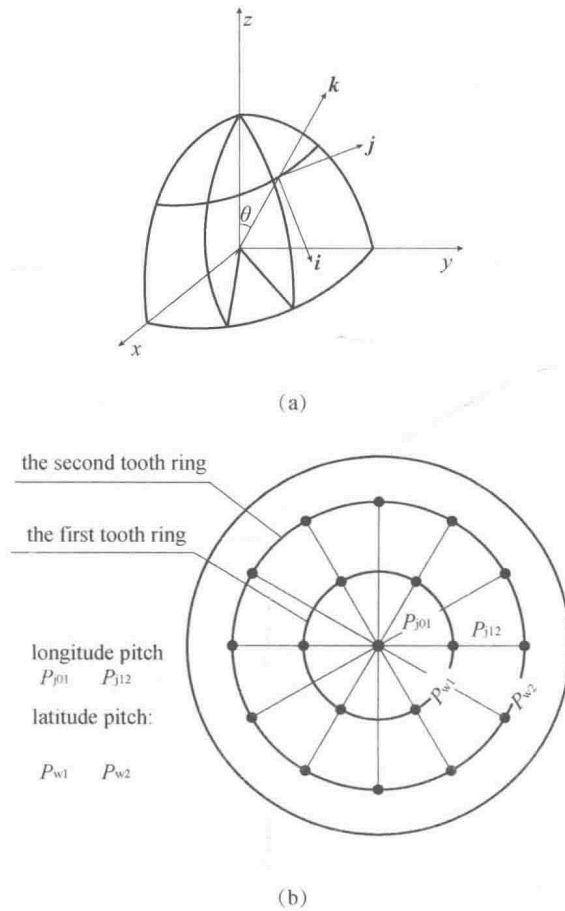


Fig. 4 The distribution of teeth

Put a tooth in the centre of Fig. 4 (b); Distribute six teeth evenly on the first ring of latitude and twelve on the second one. To one certain tooth on the pitch sphere, its tooth profile equation will be established in the local space rectangular coordinate system. The three directions of the coordinate axes in the local space rectangular coordinate system are respectively the tangent line direction i of longitude, the tangent line direction j of latitude and normal line direction k of the pitch surface.

3 GEOMETRIC CALCULATION AND THE FLANK PROFILE EQUATION FOR CONE CONVEX TEETH

The convex tooth is of cone shape with a full tooth height of H_0 and a profile angle of α . Its axial cross section is shown as in Fig. 5. The dotted line indicates the pitch spherical surface Σ_1 . Its radius is R . The flank profile of the cone convex tooth is indicated by line $ABCD$ in Fig. 5, of which AB is the addendum, and H is the distance from cone top to P point on the pitch spherical surface. In order to prevent the possible interference in the process of gear engagement, the addendum must be limited within $PK \leq H \cdot \sin^2 \alpha$. We take out a point F in the middle part of the tooth, and make $PF = m$, m is the module of the gear. Referring to the formula for tooth thickness of the involute gear, we stipulate the tooth thickness here (at F point) is $\frac{\pi}{2}m - 2\delta$, that is $EF = \frac{\pi}{4}m - \delta$, in which δ is the circumferential modification on a single side of the cone tooth (single side tooth thickness decrease). The purpose of stipulating δ is to prevent the addendum of the concave tooth becoming sharp pointed. The geometrical calculation formula for each variables are as follows

$$\left. \begin{aligned} H &= \left(\frac{\pi}{4}m - \delta \right) \cot \alpha - m \\ PK &= H \sin^2 \alpha \\ PQ &= H_0 - PK \\ AK &= H \cdot \sin \alpha \cdot \cos \alpha \end{aligned} \right\} \quad (4)$$

In Fig. 5, the equation of the flank profile in AC side is

$$\left. \begin{aligned} X_1 &= -(H - V) \tan \alpha \\ Y_1 &= R + V \end{aligned} \right\} \quad (5)$$

Here V is a variable parameter, the range of it is

$$-PQ \leq V \leq PK, \text{ at } P \text{ point, } V=0$$

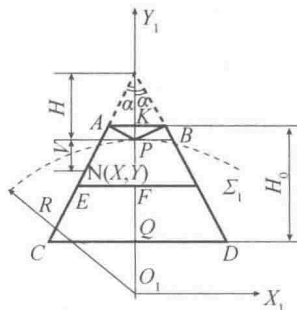


Fig. 5 A cone - shaped convex tooth

4 COORDINATE TRANSMISSION

As the above shows, the spherical gear transmission with the transmission ratio 1 is, substantially, similar to the case in which two pitch surfaces of the same size roll against one another in the limited space. No matter which pair of the convex tooth and concave tooth on the spherical surface is engaging, their transmission ratio is always equal to 1. Therefore each pair of the convex tooth and concave tooth on the spherical surface engages exactly in the same way. When the flank profile of convex tooth is a rotative surface—a cone surface, the flank profile of the concave tooth is also a rotative surface. So it is typical to study the flank profile of any pair of a convex tooth and a concave tooth, when they are engaging along the longitudinal dissection on the pitch curve surface. The engagement of the convex tooth and concave tooth along the longitudinal direction of the pitch surface is equivalent to the engagement of a pair of cylinder gear with a transmission ratio 1. Therefore, we can make use of the solution for flank profile of the cylinder gear at the engagement to obtain the tooth shape of the concave tooth.

In Fig. 6, 1 and 2 are two pitch circles with the same radius. P is the pitch point. The centers of the two pitch circles are O_1 and O_2 respectively. The central distance is $a = 2R = O_1O_2$, the coordinate system $X_1O_1Y_1$ is fixed on gear 1; $X_2O_2Y_2$ is fixed on gear 2, XOY is a motionless coordinate system. The initial position of Y_1 , Y_2 and Y coincides with each other. $X_gO_gY_g$ is fixed with coordinate system $X_2O_2Y_2$. O_g is on pitch circle 2. In the coordinate system $X_gO_gY_g$, the flank profile equation for concave tooth and its coordinate value will be more direct. The radius of addendum circle of the concave tooth is R_{a2} (dotted line in Fig. 6). The relationship between those concerned coordinates are as follows

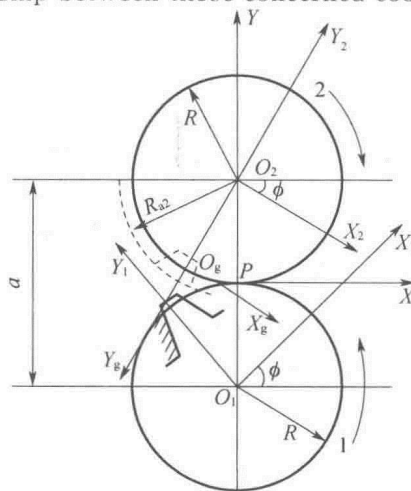


Fig. 6 Definition of coordinate systems

$$\begin{pmatrix} X \\ Y \\ 1 \end{pmatrix} = \mathbf{M}_{01} \cdot \begin{pmatrix} X_1 \\ Y_1 \\ 1 \end{pmatrix} = \begin{pmatrix} \cos\phi & -\sin\phi & 0 \\ \sin\phi & \cos\phi & -R \\ 0 & 0 & 1 \end{pmatrix} \cdot \begin{pmatrix} X_1 \\ Y_1 \\ 1 \end{pmatrix} \quad (6)$$

$$\begin{pmatrix} X_2 \\ Y_2 \\ 1 \end{pmatrix} = \mathbf{M}_{20} \cdot \begin{pmatrix} X \\ Y \\ 1 \end{pmatrix} = \begin{pmatrix} \cos\phi & -\sin\phi & R\sin\phi \\ \sin\phi & \cos\phi & -R\cos\phi \\ 0 & 0 & 1 \end{pmatrix} \cdot \begin{pmatrix} X \\ Y \\ 1 \end{pmatrix} \quad (7)$$

$$\begin{aligned} \begin{pmatrix} X_2 \\ Y_2 \\ 1 \end{pmatrix} &= \mathbf{M}_{21} \cdot \begin{pmatrix} X_1 \\ Y_1 \\ 1 \end{pmatrix} = \mathbf{M}_{20} \cdot \mathbf{M}_{01} \cdot \begin{pmatrix} X_1 \\ Y_1 \\ 1 \end{pmatrix} \\ &= \begin{pmatrix} \cos 2\phi & -\sin 2\phi & a\sin\phi \\ \sin 2\phi & \cos 2\phi & -a\cos\phi \\ 0 & 0 & 1 \end{pmatrix} \cdot \begin{pmatrix} X_1 \\ Y_1 \\ 1 \end{pmatrix} \end{aligned} \quad (8)$$

$$\begin{pmatrix} X_g \\ Y_g \\ 1 \end{pmatrix} = \mathbf{M}_{g2} \cdot \begin{pmatrix} X_2 \\ Y_2 \\ 1 \end{pmatrix} = \begin{pmatrix} 1 & 0 & 0 \\ 0 & -1 & -R \\ 0 & 0 & 1 \end{pmatrix} \cdot \begin{pmatrix} X_2 \\ Y_2 \\ 1 \end{pmatrix} \quad (9)$$

5 THE EQUATION FOR CONTACTING LINE AND THE EQUATION FOR THE FLANK PROFILE OF THE CONCAVE TOOTH

The equation for contacting line

$$\left. \begin{aligned} X &= X_1 \cos\phi - Y_1 \sin\phi \\ Y &= X_1 \sin\phi + Y_1 \cos\phi - R \end{aligned} \right\} \quad (10)$$

The equation for the flank profile of the concave tooth

$$\left. \begin{aligned} X_2 &= X_1 \cos 2\phi - Y_1 \sin 2\phi + a \sin\phi \\ Y_2 &= X_1 \sin 2\phi + Y_1 \cos 2\phi - a \cos\phi \end{aligned} \right\} \quad (11)$$

6 THE CALCULATION IN COORDINATES FOR THE FLANK PROFILE OF THE CONCAVE TEETH

Take as a typical example the engagement of the left side flank of the central convex tooth (the shadow part in Fig. 6) and the corresponding flank profile of the central concave tooth. According to the given shape of convex tooth, the shape of the concave

tooth can be identified with the method of tooth shape normal line (see document [3]) .

If the angle between axle X_1 and the tangent of convex tooth flank is γ , then

$$\tan\gamma = \frac{dY_1/dV}{dX_1/dV} = \cot\alpha \tag{12}$$

$$\cos\psi = \frac{1}{R} (X_1 \cos\gamma + Y_1 \sin\gamma) \tag{13}$$

$$\phi = \frac{\pi}{2} - (\gamma + \psi) \tag{14}$$

To get the coordinate of the flank profile of the concave tooth, the angle ϕ corresponding to the start and end position in engagement must be determined.

Suppose the addendum sphere radius of spherical gear 2 where the concave tooth located is

$$R_{a2} = R + 2m - \Delta R \tag{15}$$

Here, ΔR is the decreased amount of the addendum sphere radius of concave tooth. The purpose of setting ΔR is to prevent the addendum of the concave tooth becoming sharp pointed (within the permissible range of overlapping) .

When the root of convex tooth contacts the addendum of concave tooth, it means that a pair of teeth starts to be engaging; when the addendum of convex tooth contacts the root of concave tooth, the pair of teeth is out of engagement.

As for the engagement of central convex tooth and central concave tooth, the position at $\phi=0$ is the position of the two central teeth being out of engagement. This is determined by the convex tooth shape (cone tooth) and the position of convex tooth relative to the pitch surface Σ_1 .

It can be seen in Fig. 6 that the corresponding angle ϕ should be negative, when the central convex tooth and central concave tooth are entering the engagement position. This negative number can be obtained through solving the non-linear equation (16), in which ϕ is dealt with as an unknown number

$$X_2^2 + Y_2^2 - (R + 2m - \Delta R)^2 = 0 \tag{16}$$

Presume angle ϕ is ϕ_{in} when the central teeth begin to engage with one another, and ϕ_{out} when they begin to go out of engagement. Then within the engaging area ($\phi_{in} \sim \phi_{out}$), give ϕ a series values, ϕ_i ($i=1, 2, \dots, n$) at a set step, a series of coordinate values of concave - tooth flank profile can be worked out according to the following procedures

